Human Molecular Genetics, 2014, Vol. 23, No. 17 **4569–4580**
doi:10.1093/hmg/ddu170
Advance Access published on April 9, 2014

Competing targets of microRNA-608 affect anxiety and hypertension

Geula Hanin[1,2], Shani Shenhar-Tsarfaty[1,2], Nadav Yayon[1,2], Yin Hoe Yau[3], Estelle R. Bennett[1,2], Ella H. Sklan[4], Dabeeru. C. Rao[5], Tuomo Rankinen[6], Claude Bouchard[6], Susana Geifman-Shochat[3], Sagiv Shifman[1], David S. Greenberg[1,2] and Hermona Soreq[1,2,*]

[1]The Silberman Institute of Life Sciences and [2]The Edmond and Lily Safra Center for Brain Sciences, The Hebrew University of Jerusalem, The Edmond Safra Campus, Givat Ram, Jerusalem 91904, Israel, [3]School of Biological Sciences, Nanyang Technological University, 60 Nanyang Avenue, 637551, Singapore, [4]Department of Clinical Microbiology and Immunology, Sackler School of Medicine, Tel Aviv University, Tel Aviv 69978, Israel, [5]Division of Biostatistics, School of Medicine, Washington University in St. Louis, St. Louis, MO, USA and [6]Human Genomics Laboratory, Pennington Biomedical Research Center, Baton Rouge, LA, USA

Received January 14, 2014; Revised March 4, 2013; Accepted April 8, 2014

MicroRNAs (miRNAs) can repress multiple targets, but how a single de-balanced interaction affects others remained unclear. We found that changing a single miRNA–target interaction can simultaneously affect multiple other miRNA–target interactions and modify physiological phenotype. We show that miR-608 targets acetylcholinesterase (AChE) and demonstrate weakened miR-608 interaction with the rs17228616 AChE allele having a single-nucleotide polymorphism (SNP) in the 3′-untranslated region (3′UTR). In cultured cells, this weakened interaction potentiated miR-608-mediated suppression of other targets, including CDC42 and interleukin-6 (IL6). Postmortem human cortices homozygote for the minor rs17228616 allele showed AChE elevation and CDC42/IL6 decreases compared with major allele homozygotes. Additionally, minor allele heterozygote and homozygote subjects showed reduced cortisol and elevated blood pressure, predicting risk of anxiety and hypertension. Parallel suppression of the conserved brain CDC42 activity by intracerebroventricular ML141 injection caused acute anxiety in mice. We demonstrate that SNPs in miRNA-binding regions could cause expanded downstream effects changing important biological pathways.

INTRODUCTION

MiRNAs are short non-coding RNAs, 20–25 nucleotides long, that can simultaneously regulate multiple genes in biological pathways (1) by post-transcriptionally suppressing translation and/or inducing degradation of their mRNA targets (1–3), suggesting that they are particularly suitable for controlling the rapidly adjustable physiology of the parasympathetic system. Moreover, owing to the multileveled activities of Acetylcholine (ACh) signaling, miRNAs could modulate both the neuronal and immune functions of ACh by controlling its production and elimination (4,5). However, the biological impact of maintaining multiple miRNA–target interactions balanced the inherited diversity of miRNA regulation or how impairments in one interaction would affect the others has not been thoroughly addressed (5).

Single-nucleotide polymorphism (SNP) interference with miRNA functions affects the expression of corresponding targets, modifies brain functions and induces a risk of disease. In Tourette's syndrome, a 3′UTR SNP in the brain-expressed human Slit and Trk-like-1 (SLITRK1) gene strengthens an existing miRNA-189 target site (6), and an A1166C SNP in the angiotensin receptor 1 (AGTR1) gene abrogates its miRNA-155-mediated regulation, exacerbating the risk of hypertension and cardiovascular disease (7). Nevertheless, whether these phenotypes reflect mis-regulation of other targets was scarcely addressed. An exception is the pseudogene PTENP1 whose homology to the 3′UTR region of the cognate PTEN gene

*To whom correspondence should be addressed. Tel: +97226585109; Fax: +972 26520258; Email: hermona.soreq@mail.huji.ac.il

enables it to interact with and de-repress targets of the authentic PTEN-targeting miRNAs (8). This suggests that both coding and non-coding RNA targets that share miRNA response elements can compete for miRNA binding (9,10), as was demonstrated in plant starvation for miR-399 (11), but thoroughly tested examples for such competition in humans are still lacking.

In both the nervous and the immune system, the ACh-hydrolyzing enzyme acetylcholinesterase (AChE) is targeted by miR-132, which controls inflammation (4). This regulation is disturbed in numerous syndromes, including Alzheimer's disease (12), inflammatory bowel disease (13) and acute stress (14), suggesting that inherited and/or acquired interference with AChE-targeted miRs may change the outcome of diverse anxiety and inflammation-related diseases. Recently, we identified the primate-specific miR-608 (14) as a potential AChE-targeting miRNA. MiR-608 is encoded by an intron of the SEMA4G gene, a member of the immunoglobulin family (15) the promoter of which includes inflammation and stress-related motifs (Supplementary Material, Fig. S1A). We hypothesized that the miR-608 multi-target effects would be particularly important for parasympathetic and anxiety-controlling genes participating in brain-to-body communication (4,14,16,17) (Fig. 1A). Therefore, we used this case to test the impact of the AChE 3′UTR rs17228616 SNP (18) (www.ncbi.nlm.nih.gov/projects/SNP) located at the AChE-binding site with the primate-specific miR-608 on its interactions with the validated CDC42 (19) and interleukin-6 (IL6) (20) targets *in vitro* and *in vivo* and the consequences of changes in these interactions.

RESULTS

The primate-specific miR-608 is a bona fide miRNA that targets the major rs17228616 AChE allele

The 3′UTR C2098A substitution (rs17228616) is located in the 'seed'-interacting region of a putative AChE-binding site to miR-608 (18,21), close to the binding site of the AChE-targeting miR-132 (4) (Fig. 1B and C). However, miR-608 is unusually long (25 nucleotides), and reports of its miRNA activity were limited to heterologous systems. Therefore, we used quantitative RT-PCR to interrogate the *in vivo* expression of miR-608. These tests revealed high, medium and insignificant expression of miR-608, validated by sequencing in human intestine, brain and white blood cells (Fig. 1D and Supplementary Material, Fig. S1B). Furthermore, miR-608 was efficiently co-precipitated with AGO2, identifying it as a genuine bona fide miRNA, which functions via the AGO2 complex in spite of its being 25 nucleotides long (Fig. 1E). To test the predicted miR-608–AChE interaction, we cloned the AChE 3′UTR into a MicroRNA Target Selection vector carrying an upstream cytotoxic sensor and firefly luciferase, stably transfected human embryonic kidney 293T(HEK-293T) cells and infected these cells with miRNA-expressing lentiviruses. Cells expressing either miR-608 or miR-132 survived and showed 55 and 45% reduction in luciferase activity, respectively ($n = 6$, one-way ANOVA: $P = 0.01$, $P = 0.008$, Fig. 1F), reflecting functional miRNA–target interactions, whereas cells infected with a negative control lentivirus died (Supplementary Material, Fig. S1C and D). Also, human-originated U937 cells infected with miR-608 or miR-132 lentiviruses secreted less endogenous AChE compared with controls (by 21.4 and 15.1%, respectively, $n = 5$, one-way ANOVA: $P = 0.007$, $P = 0.003$). Both catalytic AChE activities and AChE protein levels in U937 cells infected with miR-608 or miR-132 lentiviruses were substantially reduced ($n = 3$, one-way ANOVA: $P = 0.024$, $P = 0.026$, Fig. 1G), together validating AChE and the cholinergic signaling pathway as being targeted by miR-608. Moreover, transfecting the AChE non-expressing 293T cells (21) to carry comparable copy numbers of the major or the minor rs17228616 allele (Supplementary Material, Fig. S1E) showed reduced luciferase activity under co-transfection with miR-608 by the major, but not the minor AChE 3′UTR allele (by 44%, $n = 5$, one-way ANOVA: $P < 0.001$) (Fig. 1H and Supplementary Material, Fig. 1F and G), indicating that the minor allele of rs17228616 reduces miR-608–AChE interaction.

Quantifying miR-608 interaction with its targets

Predictably, miR-608 shows thousands of potential targets (miRNAwalk: http://www.umm.uni-heidelberg.de/apps/zmf/miRNAwalk). Of those, the validated miR-608 targets Rho GTPase CDC42 (19) and IL6 (20) are predictably involved in anxiety and parasympathetic signaling. Bioinformatics analysis (RNAhybrid, http://bibiserv.techfak.uni-bielefeld.de/rnahybrid/) predicted relatively tight binding to miR-608 for the C-allele and the A-allele sequences (−31.4 and −25.8 Kcal/mol), CDC42 (−26.4 Kcal/mol) and miR-132–AChE interaction (−17.3 Kcal/mol) (Fig. 2A and B). To experimentally measure miR-608–target association, we adapted an *in vitro* surface plasmon resonance (SPR) assay (22) for hybridization tests. Given that miRNA–target interactions may involve longer regions than the seed itself (1), we immobilized biotin-linked 30-mer RNA sequences of the corresponding regions in the major C-allele of AChE or CDC42 to SPR chips and injected a 25-mer RNA oligonucleotide with the miR-608 sequence. This demonstrated a ∼15-fold reduction in the affinity of miR-608 to the minor A-allele compared with the C-allele AChE sequences (K_D of 50.9 versus 3.1 nM, Fig. 2C and D and Supplementary Material, Fig. S1H), indicating weakened A-allele AChE–miR-608 interaction. CDC42-miR-608 and AChE–miR-132 presented intermediate affinities (15.8 and 18.8 nM, Fig. 2E and F), predicting a hierarchical binding preference of miR-608 to the C-allele AChE, CDC42 and the A-allele AChE target sites (Fig. 2G and H).

The minor rs17228616 allele weakens AChE suppression while potentiating suppression of other miR-608 targets

The impaired interaction of the A-allele AChE with miR-608 predicted both weakened AChE suppression and more miR-608 molecules free to suppress other targets with tighter binding parameters, such as CDC42 and IL6 (Fig. 3A). Indeed, miR-608-transfected HEK-293T cells carrying the minor A-allele AChE 3′UTR showed intensified CDC42 suppression compared with those carrying the major C-allele ($n = 6$, one-way ANOVA: $P < 0.05$, Fig. 3B). Furthermore, miR-608 dose-dependence experiments showed increasing reductions in both AChE and CDC42 mRNA, while demonstrating that the A-allele AChE is less susceptible to miR-608 suppression and that its presence leads to enhanced suppression of CDC42

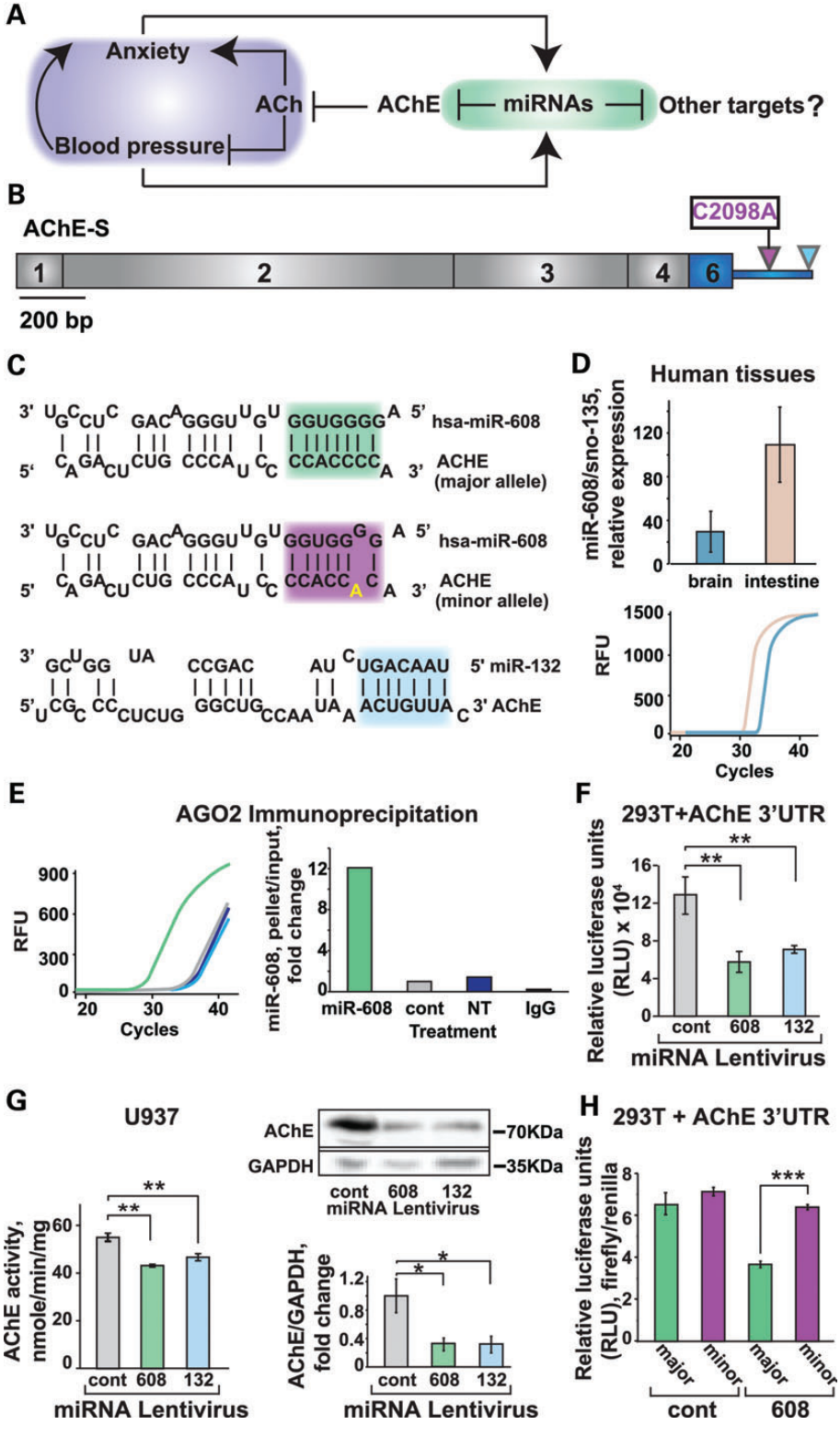

Figure 1. miR-608 targets the major rs17228616 AChE allele. (**A**) AChE–miRNA interactions predictably modify ACh signaling, anxiety and blood pressure. (**B**) Synaptic AChE mRNA (AChE-S), with the C2098A SNP in its 3′-untranslated region. (**C**) Complementary AChE alleles, miR-608 and miR-132 sequences. Seed regions are colored and the SNP marked in yellow. (**D**) Endogenous expression of miR-608 in human brain and intestine tissues. (**E**) miR-608 expression in RNA extracted from AGO2 immunoprecipitation of extracts from HEK-293T cells stably expressing AChE 3′UTR and transfected with miR-608, control plasmid (cont) or non-treated (NT). (**F**) Luciferase activity of HEK-293T cells stably expressing luciferase-AChE 3′UTR and infected with miR-132, miR-608 or control lentiviruses. (**G**) AChE activity and representative immunoblot and quantification in human U937 lentivirus-infected U937 cells. (**H**) Luciferase activity of HEK-293T cells stably expressing luciferase-linked major or minor rs17228616 AChE 3′UTR alleles and infected with either miR-608 or control lentiviruses.

A

miR-608	AGGGGUGGUGUUGGGACAGCUCCGU
AChE (C allele) binding site to miR-608	CCCCAGACUCUGCCCAUCCCCACCCCACC
AChE (A allale) binding site to miR-608	CCCCAGACUCUGCCCAUCCCCACCACACC
CDC42 binding site to miR-608	GCCUCUGCGUCUUUUUACUCACCACCUUAG
miR-132	UAACAGUCUACAGCCAUGGUCG
AChE binding site to miR-132	CUGGGCCGCCAAUAAACUGUUACAGCCACC

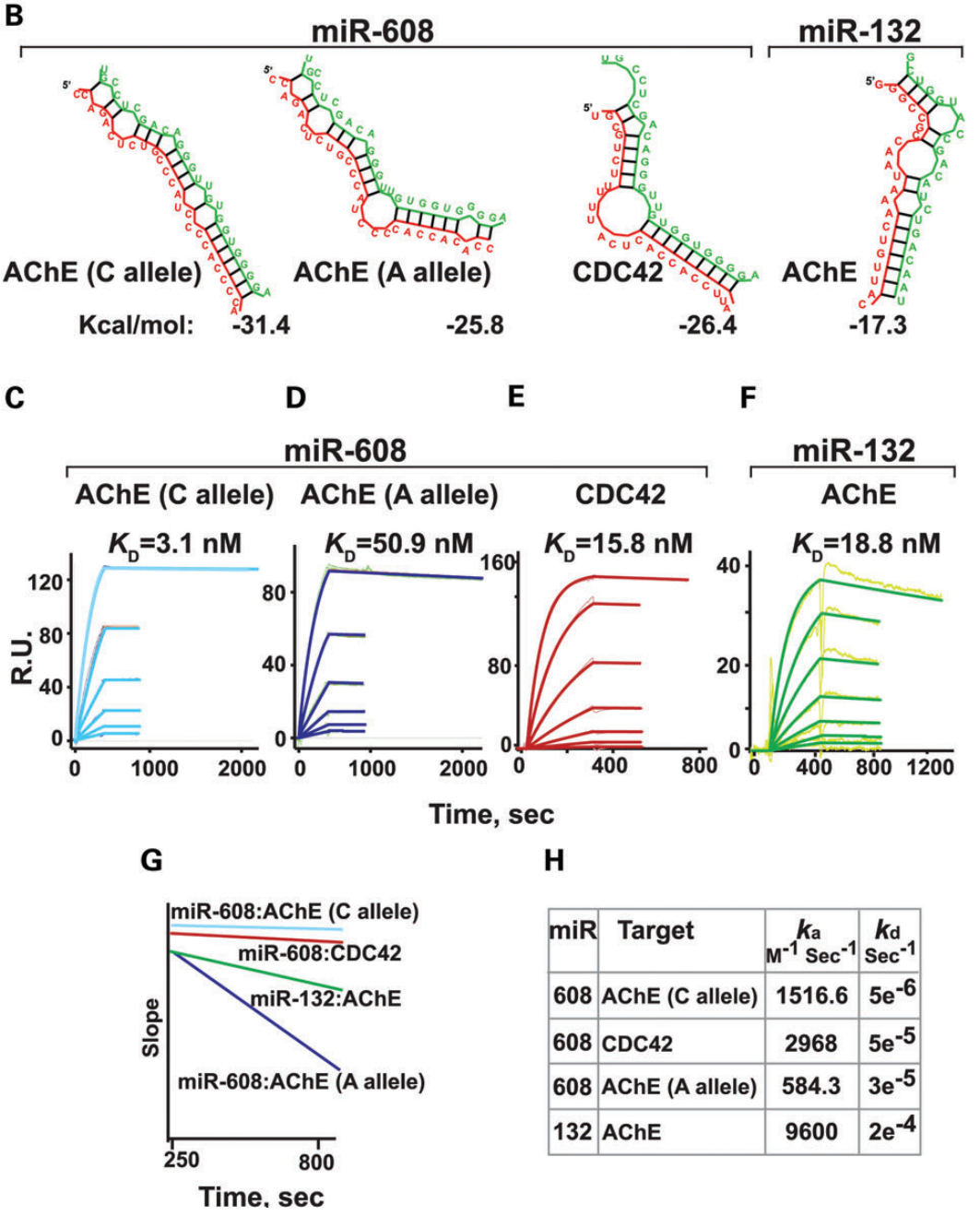

miR	Target	k_a M^{-1} Sec^{-1}	k_d Sec^{-1}
608	AChE (C allele)	1516.6	$5e^{-6}$
608	CDC42	2968	$5e^{-5}$
608	AChE (A allele)	584.3	$3e^{-5}$
132	AChE	9600	$2e^{-4}$

Figure 2. Quantified miR-608–target interactions. (**A**) Target and miRNA RNA oligonucleotides sequences. Seed regions are colored. (**B**) Predicted structures and binding energy of miR-608 with AChE's C-allele and A-allele and CDC42, and of miR-132 with AChE. (**C**–**E**) SPR sensograms showing binding of miR-608 to the C-allele and A-allele of AChE and CDC42 targets. Biotinylated target RNA oligonucleotides were immobilized to a streptavidin chip, and increasing concentrations (0.3125, 0.625, 1.25, 2.5, 5 and 10 μM) of miRNA oligonucleotides were injected over the chip. (**F**) SPR sensorgrams showing miR-132–AChE binding. (**G**) SPR dissociation slopes of the indicated interactions. (**H**) k_a and k_d values for the SPR reactions.

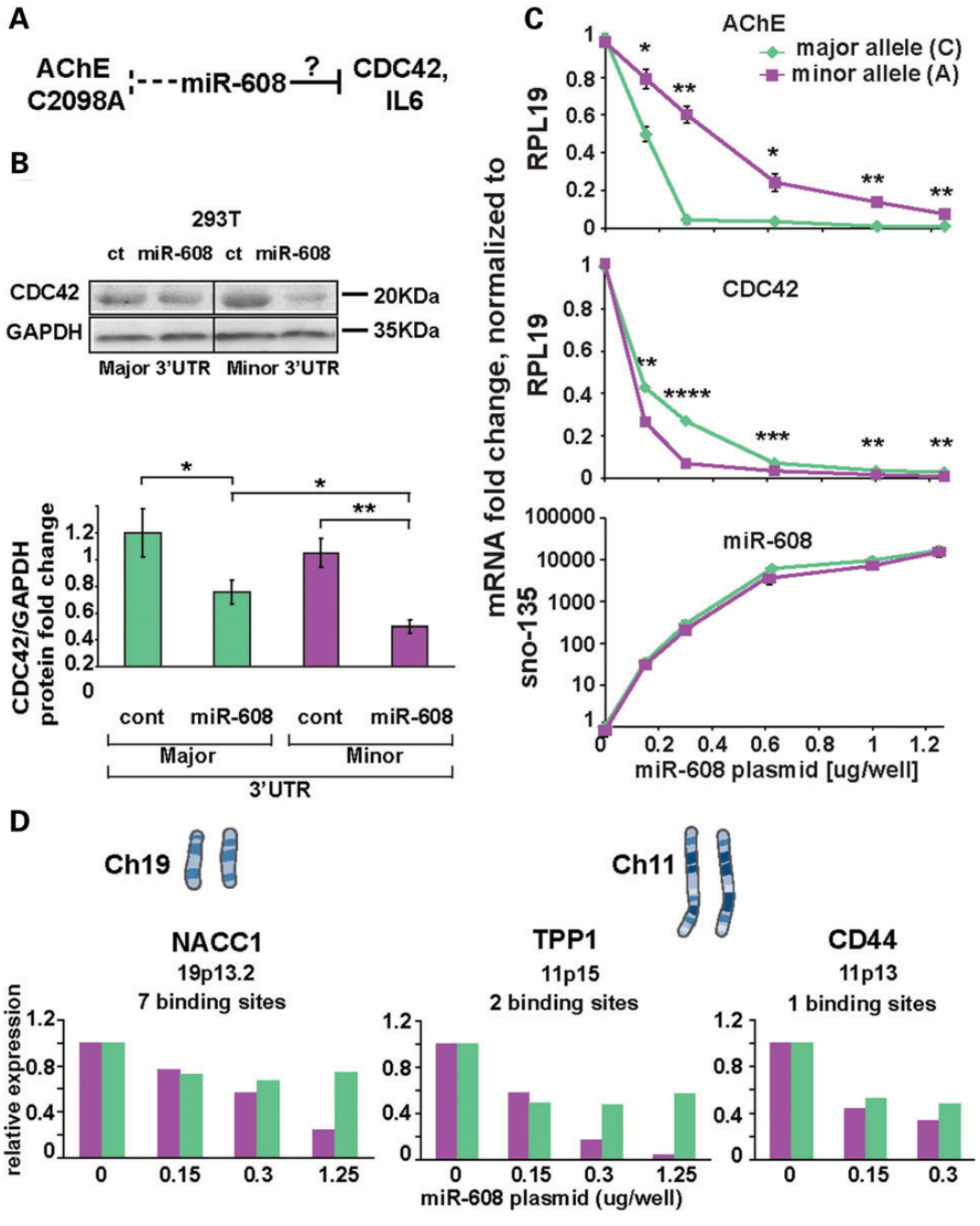

Figure 3. Cells carrying the minor rs17228616 allele show limited suppression of AChE and potentiated suppression of CDC42, IL6 and other predicted targets. (**A**) Experimental hypothesis: weakened miR-608–AChE C2098A interaction would modify CDC42 and IL6 suppression. (**B**) A representative immunoblot and quantification of CDC42 and GAPDH in HEK-293T cells stably expressing the two AChE alleles, transfected with miR-608 or control plasmids. $N = 3$ experiments, each in duplicates or triplicate. (**C**) RNA levels of AChE, CDC42 and miR-608, as a function of miR-608 plasmid dosage (range: 0 to 1.25 ug, in triplicates or duplicates); $n = 3$ experiments. (**D**) RNA levels of NACC1, TPP1 and CD44 by miR-608 obtained in a Fluidigm test of pooled samples as in C.

compared with the C-allele 3′UTR, under conditions of unchanged miR-608 levels ($n = 5$, Student's t-test: $P < 0.05$ per dosage, Fig. 3C). To test the hypothesis that parallel effects exist for additional miR-608 targets, we identified the top predicted targets of miR-608 by multiple algorithms according to the miRwalk database (http://www.umm.uni-heidelberg.de/apps/zmf/mirwalk/) and designed a microfluidics dynamic array experiment (Fluidigm, http://www.fluidigm.com/biomark-hd-system.html) to simultaneously and comparatively quantify changes in those predicted targets that are expressed in these cells (raw data in Supplementary Material, Table S2). Three of the tested genes showed parallel differences to those observed for CDC42 and IL6. These were NACC1, mapped to Chromosome 19p13.2, known to alter the HMGB1-mediated autophagic response (23) and carrying seven predicted binding sites for miR-608; the Chromosome 11p15 TPP1 tripeptidyl-peptidase 1 lipid metabolism-regulating enzyme (24), with two predicted sites for miR-608; and the Chromosome 11p13

validated angiogenesis regulating target CD44 (19), with one binding site for miR-608. Enhanced suppression of each of these putative target genes in cells carrying the A-allele compared with the C-allele (Fig. 3D) demonstrated that this effect extends beyond CDC42 and IL6 differences and that it occurs in transcripts of different chromosomal origins carrying different numbers of miR-608-binding sites.

The A-allele is relatively abundant, particularly in African-originated populations [Frequency in African ancestry (YRI, HapMap population) = 0.323; in Europeans (CEU) = 0.04]. In the human brain, both CDC42 and IL6 are involved in the anxiolytic GABAergic neurotransmission and inflammatory reactions, respectively (25–27). Given the neuroimmune activities of AChE-targeting miRNAs (4,5,14,21), we compared the effects of rs17228616 on CDC42 and IL6 levels in adult entorhinal cortices from The Netherlands Brain Bank (28). DNA sequencing identified three matched pairs of apparently healthy homozygotes for the minor and major rs17228616 alleles (Fig. 4A and Supplementary Material, Table S3), with indistinguishable miR-608 levels (Fig. 4B). However, brain samples homozygous for the minor allele (AA) presented 65% more hydrolytic activity of AChE (Student's *t*-test: $P < 0.05$) than homozygote major allele tissues (CC). The homologous enzyme butyrylcholinesterase (BChE) (29) showed no differences in these six samples (Fig. 4C and D), demonstrating specificity. Moreover, immunoblots showed lower levels of IL6 and CDC42 in tissues homozygous for the minor compared with the major allele (Student's *t*-test: $P < 0.05$ for both, Fig. 4E–G), indicating that A-allele-related weakening of AChE suppression can increase the suppression of other miR-608 targets in the adult human brain.

CDC42, IL6 and AChE are all causally involved with anxiety (25,26,30,31). Specifically, AChE up-regulation in anxiety (32,33) could suppress ACh levels, intercepting ACh blockade of inflammation (30), whereas the miR-608 target CDC42 interacts with collybistin in GABAergic neurons and is actively involved in the formation of the anxiolytic $GABA_A$ receptor synapse (25,34). Therefore, we predicted that rs17228616 causes additive cholinergic and GABAergic pathway-mediated increases in anxiety and parasympathetic signaling. This should impair the sympathetic control of blood pressure (35) and modify parasympathetic and anxiety phenotypes (25,33,36–38) in minor allele heterozygotes and homozygotes.

Human volunteers with the minor rs17228616 allele show elevated blood pressure and reduced cortisol

The HERITAGE Family Study cohort (HEalth, RIsk factors, exercise Training And GEnetics) recruited young, healthy adults, of Caucasian or African-American ethnic origins (36) (see Supplementary Material, Tables S4 and S5 for population characteristics). Genotyping indicated that this cohort includes 63/159 and 13/209 homozygotes or heterozygotes for the minor A-allele in the African-American and Caucasian groups, respectively (Fig. 5A). Separate association analysis for the African-American and Caucasian datasets was then combined using meta-analysis. Volunteers homozygous and heterozygous for the minor A-allele showed sharply reduced serum cortisol levels and higher, albeit non-pathological systolic and diastolic blood pressure compared with homozygotes of the major C-allele ($P = 9.77 \times 10^{-8}$, $P = 0.05$, $P = 0.0031$, Fig. 5B–D and Supplementary Material, Fig. S2), in spite of their young age and generally good health (36). Reduced circulating cortisol and elevated blood pressure are known factors predicting increased risks of both anxiety and hypertension-related diseases (39,40). Also, a genome-wide association study in African-Americans reported significant association with hypertension for another SNP, rs78011900, in full linkage disequilibrium with rs17228616 (41).

Inhibiting brain CDC42 causes anxiety in mice

MiR-608 is a primate-specific miRNA that does not exist in mice, but its CDC42 target (19) is expressed in the mouse brain. To test whether the CDC42 suppression caused by the rs17228616 minor allele is anxiogenic, we intracerebroventricularly injected C57Bl/6J mice with increasing doses of the CDC42 inhibitor ML141 (42), until reaching a sufficient dose causing 40% decrease in its GTPase activity and mimicking the outcome in minor allele carriers (Fig. 6A and B, $n = 5$, Student's *t*-test: $P = 0.0002$). After 24 h, ML141-injected mice spent less time than saline-injected controls in the anxiogenic center of an open field, preferring its periphery (Fig. 6C and D, $n = 7$, Student's *t*-test: $P < 0.01$ in all cases). Treated mice traveled similar distances, excluding motor impairments or loss of general drive (Fig. 6E and F) but avoided open arms and preferred closed arms in an elevated plus maze (Fig. 6G and H, Student's *t*-test: $P < 0.001$, $P < 0.01$), suggesting anxiogenic reaction to CDC42 suppression.

DISCUSSION

We selected the primate-specific miR-608–AChE interaction, which is naturally impaired in heterozygotes and homozygotes for the minor AChE rs17228616 allele as a case study for assessing the hierarchic potency of this specific interaction over cholinergic/parasympathetic signaling and anxiety. We established the role of miR-608 as a functioning suppressor of AChE by qPCR sequencing, SPR, luciferase and AChE activity and cell survival assays. In cultured cells and human cortices expressing the minor rs17228616 allele, we showed potentiated miR-608 suppression of CDC42 and IL6. Excessive suppression of CDC42 caused acute anxiety, supporting the notion that this could be an underlying pathway; and microfluidics dynamic array tests showed enhanced suppression of the validated miR-608 target CD44 and the predicted NACC1 and TPP1 targets in cells carrying the minor (A) compared with the major (C) allele. CD44 is known for its involvement in hematopoietic tumors (19), NACC1 is involved in proliferation, apoptosis and transcriptional regulation (23) and TPP1 functions in the lysosome to cleave N-terminal tripeptides (24), suggesting potentially wider implications of rs17228616 in cancer and neurodegenerative disease. Supporting this notion, young, healthy volunteers with the minor rs17228616 allele show elevated blood pressure and reduced cortisol, predicting risk of aging-related diseases. Taken together, these findings suggest that singly impaired miR-608–AChE interaction exacerbates the suppression of CDC42, IL6, CDC44 and possibly other targets, increasing inherited risks of anxiety and hypertension (Fig. 6I).

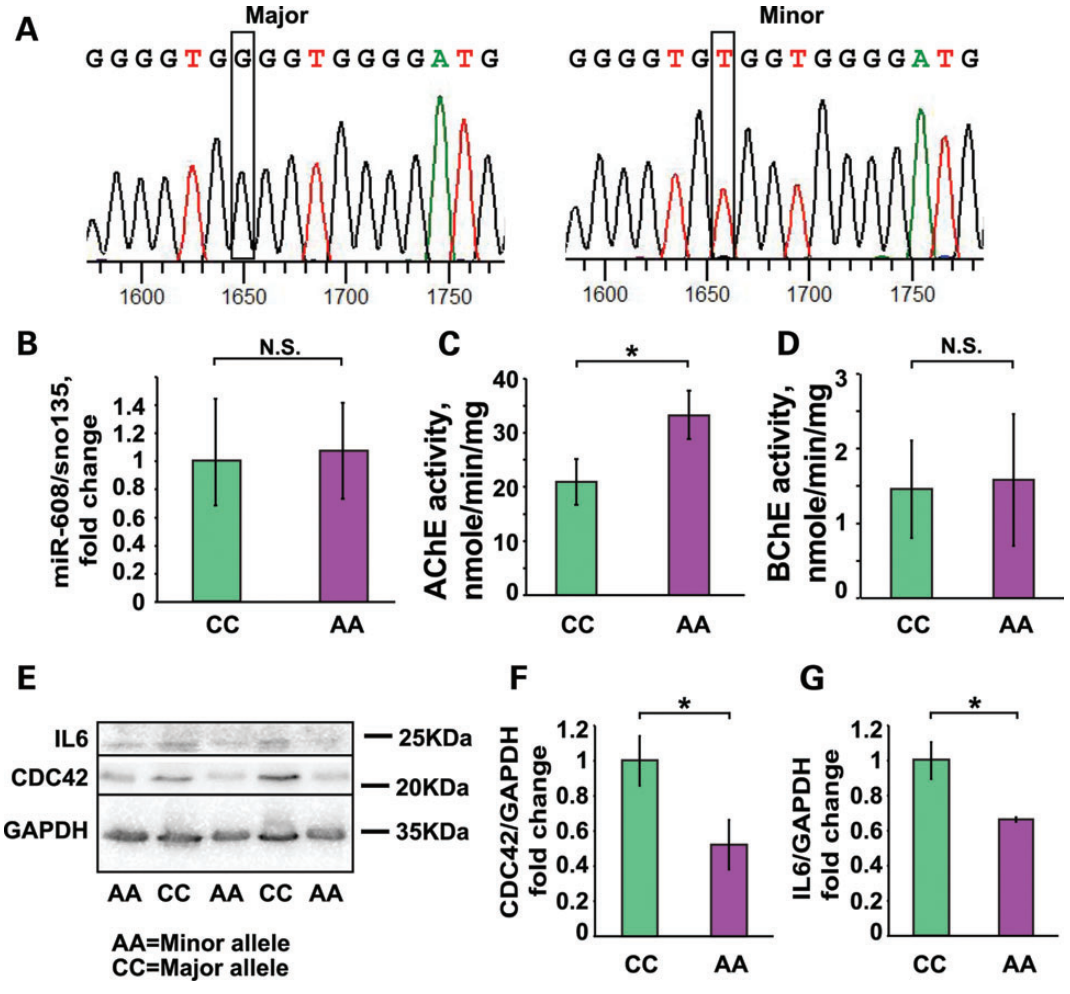

Figure 4. Human brain samples carrying the minor rs17228616 allele show elevated AChE and suppress CDC42 and IL6. (**A**) Genotyped sequences of the two AChE alleles in human brain tissues. (**B**) Similar brain miR-608 levels in homozygous samples of both AChE alleles. (**C** and **D**) Elevated AChE but not BChE activity, in brain tissues from minor allele homozygotes. (**E**–**G**) Reduced CDC42 and IL6 in brains tissues homozygous for the minor allele.

Our study draws attention to the evolutionary importance of co-regulated changes in primate-specific miRNAs and their targets for higher brain functions at large (43) as well as to miRNA regulation of cholinergic signaling (44) and the elusive links between hypertension, anxiety and other diseases. Elevated blood pressure often results in generalized vascular disease (45), stroke (46) and dementia (47), and thus, it is a major risk factor for death. Moreover, the individual tendency to exhibit abnormally enhanced responses to stressors predicts the development of later hypertension (48). Despite the plentitude of available antihypertensive drugs, recent reports demonstrate unsatisfactory response to current treatment modalities (48) and call for disease prevention based on multiple risk factor approach (49,50). Recently, it has been suggested that abnormal structure, function and connectivity within a corticolimbic neural circuit in the brain leads to 'exaggerated' cardiovascular responses to stressors. Thus, the brain may be essential to the initiation and maintenance of blood pressure (51). However, the exact relation between the neural network and cardiovascular reactivity to stress is yet to be explored. Other as-yet non-validated targets of miR-608, and downstream changes in more miRNAs and their targets could also contribute to the complex phenotype of elevated anxiety and impaired parasympathetic function, indicating that these SNPs and the corresponding miRNA–target changes also involve elevated risk of aging-related diseases [e.g. Alzheimer's disease (2,52)].

We conclude that the complexity of miRNA–target interactions can affect inherited, acquired and therapeutic interference with miRNAs, contributing to human diversities and modifying phenotypes owing to cumulative effects on multiple targets. Realizing the inherited risk of delayed diseases may highlight the importance of genome information to human health and wellbeing and promote changes in life style and preventive treatment.

MATERIALS AND METHODS

AChE SNP localization

AChE SNPs were described in Hasin *et al.* (18) and the NCBI dbSNP database (www.ncbi.nlm.nih.gov/snp) and co-localized with predicted miRNA-binding sites to AChE according to Hanin and Soreq 2011 (21).

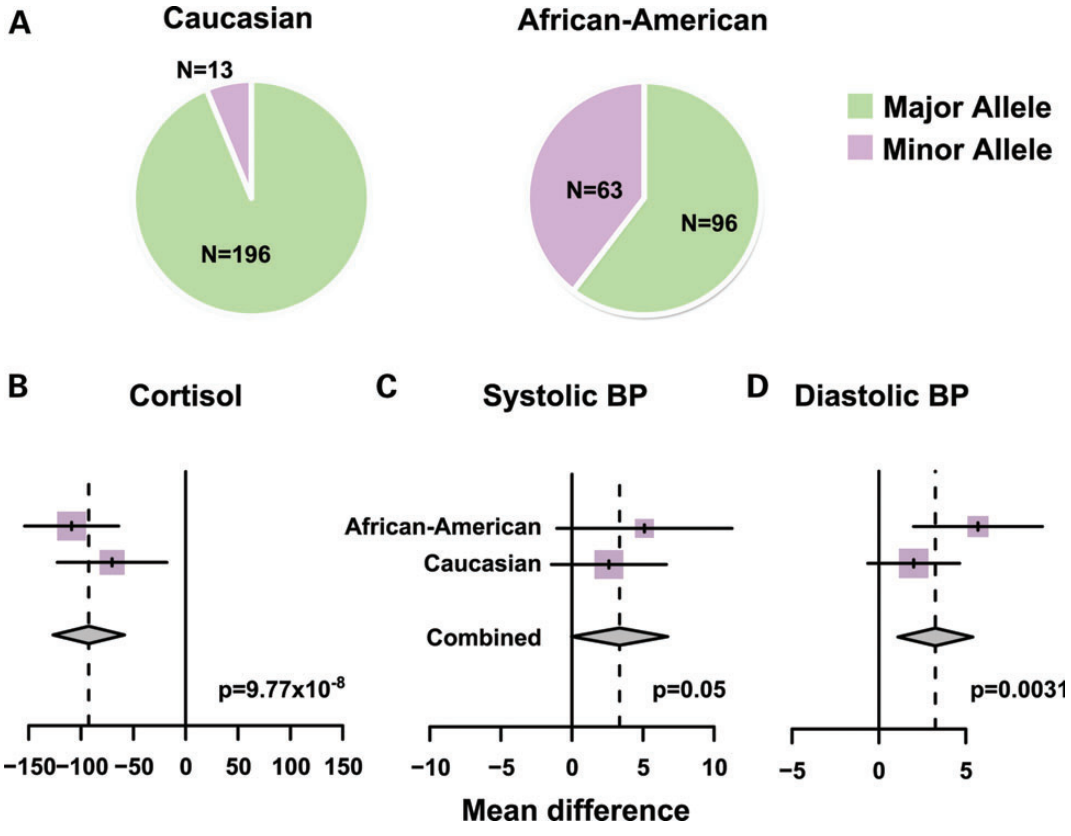

Figure 5. Healthy heterozygotes and homozygotes for the minor rs17228616 allele show reduced cortisol and elevated blood pressure. (**A**) Numbers of homozygotes for the major allele and homozygotes and heterozygotes for the minor rs17228616 allele in the HERITAGE cohort. (**B**–**D**) Meta-analysis of different ethnic origins reveals reduced serum cortisol and elevated systolic and diastolic blood pressure in heterozygotes and homozygotes for the minor allele.

Lentivirus preparation

One microgram of miRNA overexpression vectors containing pre-miR-132, -608 or a scrambled sequence (GeneCopoeia, MD, USA), 1 μg of packaging and 0.7 μg of envelope plasmid were added to serum-free Dulbecco's Modified Eagle Medium (DMEM) supplemented with 1 mM glutamine and 50 mg/ml gentamycin. HEK-293T cells were transduced using 1 mg/ml polyethylenimine (PEI) (Sigma, Israel). Virus-containing medium was collected and stored at −80°C.

Cell lines

Cells were grown in a humidified atmosphere at 37°C, 5% CO_2. U937 cells were grown in RPMI-1640 (Sigma–Aldrich), and HEK-293T cells were grown in DMEM. Media was supplemented with 10% FBS, 2 mM L-glutamine, 1000 units/ml penicillin, 0.1 mg/ml streptomycin sulfate and 0.25 microgram/ml amphotericin B (Beit-Haemek, Israel).

Cholinesterase activity

Levels of catalytic activity in human brain samples and U937 cells (assayed 96 h post-lentiviral infection) were measured using the Ellman assay as described previously (53).

Luciferase and life-death assay

AChE 3′UTR sequence was cloned into the MicroRNA Target Selection System plasmid (System Biosciences, CA, USA), a dual-luciferase reporter system. HEK-293T cells transfected with miRNA Target Selection-AChE 3′UTR were selected for 3 weeks. Stable cells were infected with miR-132, -608 or control sequence lentiviruses and supplemented with cytotoxic drug 72 h post-infection. Cell survival was determined 8 days post-infection. Luciferase activities were measured using the Dual-Luciferase® Reporter Assay (Promega, WI, USA).

Site-directed mutagenesis

The C2098A SNP AChE 3′UTR sequence (in pUC57) was constructed by mutagenesis, using the Quickchange II protocol (Stratagene, CA, USA) (Supplementary Material, Fig. S1G). Major or minor allele fragments were then cloned into the psi-CHECK2 vector (Promega).

Human samples

Blood samples and intestinal biopsies from healthy tissue samples were obtained from volunteer participants in this study; the study was approved by the ethics committee at the Tel-Aviv

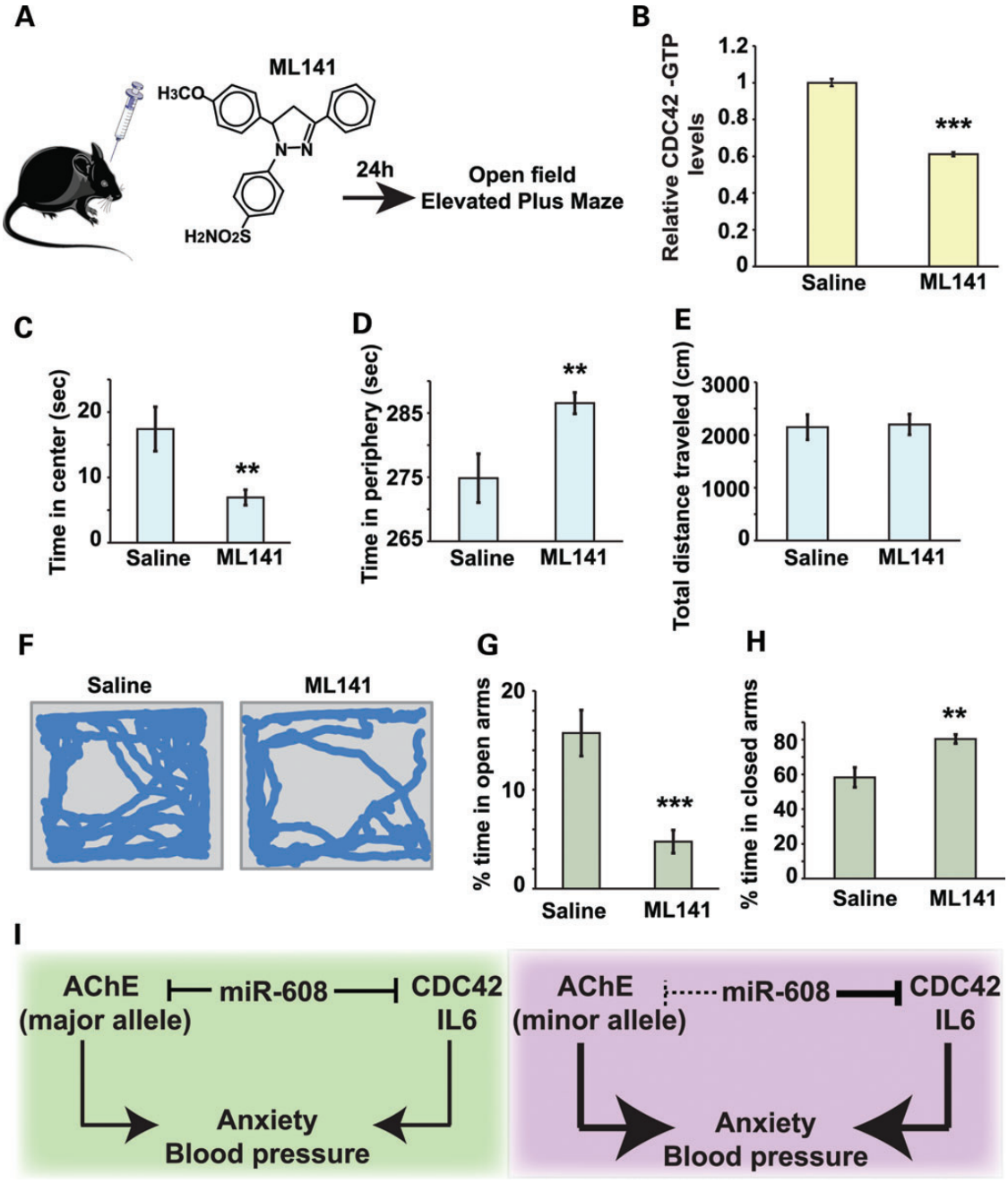

Figure 6. Brain CDC42 inhibition increases anxiety in mice. (**A**) Intracerebroventricular injection of the CDC42 inhibitor ML141 was followed by mouse anxiety and motor functioning tests. (**B**) ML141 suppresses hippocampal CDC42-GTPase activity. (**C**–**F**) ML141-injected mice prefer the periphery over the center in an open field while traveling similar distances. (**G** and **H**) ML141-injected mice prefer closed over open elevated plus maze arms. (**I**) The major AChE allele enables balanced AChE, CDC42 and IL6 levels, which together contribute to controlling anxiety and blood pressure. The minor AChE allele enhances AChE levels and reduces CDC42 and IL6, thereby dually elevating anxiety and blood pressure.

Sourasky Medical Center. Postmortem cortical samples of apparently healthy aged volunteers were obtained from The Netherlands Brain Bank (NBB, Netherlands Institute for Neuroscience, Amsterdam). All material was collected from donors from whom a written informed consent for brain autopsy and the use of the material and clinical information for research purposes had been obtained by the NBB.

AGO2 immunoprecipitation

AGO2 immunoprecipitation was performed according to Peritz *et al*. (54). AGO2 was precipitated using primary antibody (sc-32877, Santa Cruz, TX, USA, 1:200), followed by qRT-PCR using qScript microRNA quantification system (Quanta Biosciences, MD, USA).

MicroRNA-target predicted structure and binding energy

miRNA-target-binding energy and structure were predicted using the RNAhybrid algorithm (http://bibiserv.techfak.uni-bielefeld.de/rnahybrid/).

Surface plasmon resonance

Surface plasmon resonance experiments were conducted using a Biacore 3000 instrument (Biacore AB, Uppsala, Sweden). Oligonucleotides were synthesized as fully 2′O-methylated RNA. Oligos representing target mRNAs were 5′ biotinylated for immobilization to the steptavidin chips (Syntezza-IDT, Israel). All sequences appear in Figure 2. Standard buffer HBS (10 mM HEPES, 150 mM NaCl, 3.4 mM EDTA, 0.005% surfactant P20, pH 7.4) was used for the analyses carried out at 25°C. Biotinylated oligonucleotides were dissolved in 100% 1,1,1,3,3,3-hexafluoro-2-propanol to 1 mM, diluted (1:5000) into 10 mM sodium acetate pH 5.0 and injected at 10 μl/min. The levels of C-allele AChE and A-allele AChE, CDC42 and AChE–miR-132 binding site captured on the chip were 325, 305, 296 and 113 RU, respectively. MiR-608 or -132 oligos were diluted in buffer (serial two-fold dilutions, 0.3125, 0.625, 1.25, 2.5, 5 and 10 μM) and injected over the flow cells for 2 min at 10 μl/min, with 5-min association and 5-min dissociation, except for the highest concentration that was allowed to dissociate for 1 h. The sensorgrams were double-referenced and were fit using a mathematical model of a simple 1:1 interaction (Scrubber 2 software). All experiments were run in duplicate.

Immunoblots

*S*amples were lysed using a 0.01 M Tris–HCl, pH = 7.4; 1 M NaCl, 1 mM EGTA and 1% Triton X-100. SDS–PAGE separation and transfer to nitrocellulose followed standard procedures. Proteins were visualized using primary antibodies against CDC42 (ab64533, Abcam, MA, USA, 1:1000), IL6 (ab6672, Abcam, 1:1000), AChE (sc-6431, Santa Cruz Biotechnology, 1:200) and GAPDH for normalization (2118, Cell Signaling, MA, USA, 1:2000), followed by horseradish peroxidase-conjugated goat anti rabbit antibodies (Jackson Laboratories, PA, USA, 1:10 000) and enhanced chemiluminescence (EZ-ECl, Biological Industries, Beit-Haemek, Israel).

mRNA and miRNA quantification

RNA was extracted using TRI reagent (Sigma) according to the manufacturer's protocol, followed by RNA concentration measurement (Nanodrop, Thermo, Wilmington, DE, USA) and gel electrophoresis. cDNA synthesis (Promega, Madison, WI, USA) was performed, and mRNA levels were determined by quantitative real-time reverse transcriptase (ABI prism 7900HT, SYBR green master mix, Applied Biosystems, CA, USA). Primer sequences are listed in Supplementary Material, Table S1. MicroRNA levels were determined using TaqMan MicroRNA Assay (Applied Biosystems), or microRNA quantification system (Quanta Biosciences).

Human brain tissue genotyping

DNA was extracted using Direct PCR reagent (Viagen Biotech, CA, USA) supplemented with 0.3 mg/ml proteinase K (Roche, USA). Genotyping of the A-allele of rs17228616 (C2098A) versus the C-allele was performed using TaqMan genotyping primers and AccuStart genotyping ToughMix low ROX (Quanta BioSciences). To differentiate further between homozygous (AA) and heterozygous (CA) rs17228616, sequencing of PCR-amplified DNA was performed.

Fluidigm

Expression of the top predicted targets of miR-608 was determined using a high-throughput microfluidic qRT-PCR instrument (BioMark, Fluidigm, San Francisco, CA, USA). Preamplified cDNA samples were mixed with TaqMan PreAmp Master Mix (Applied Biosystems) and DDW and pipetted into the Dynamic Fluidigm Array 48 × 48 chip. Amplification reaction product was cleaned using Exonuclease I (New England Biolabs, Ipswich, MA, USA) and diluted 1:5 in Tris–EDTA buffer, pH = 8. qRT-PCR mix was prepared using 2 × SsoFast EvaGreen Supermix with low ROX (Biorad, Hercules, CA, USA). Priming and loading was performed using IFC Controller HX (BioMark). All qRT-PCR reactions were performed using the GE 48× 48 PCR + Melt v2.pcl protocol. Data analysis involved BioMark Real-Time PCR Analysis Software Version 2.0 (Fluidigm), and the ΔCt method was applied.

HERITAGE family study cohort

The Health, Risk Factors, Exercise Training, and Genetics (HERITAGE) Family Study contained a total of 461 individuals (198 men and 263 women) from 150 two-generation families of African-American (172) or Caucasian (289) origin with complete data available for this study.

Serum analyses

Blood samples were collected in the morning after a 12-h fast, and serum was separated by centrifugation at 2000 *g* (15 min at 4°C). Serum aliquots were stored at −80°C until use.

HERITAGE sample genotyping

Genomic DNA from previously screened individuals (36) was prepared from lymphoblastoid cell lines generated from HERITAGE samples. DNA genotyping was performed by the SNaPshot™ method (Applied Biosystems) and by sequencing.

Statistics

P-values for the difference between the genotypes of the subjects were calculated using the likelihood ratio test. The *P*-value was the exact conditional tail probability given the marginal, as was assessed by 100 000 Monte Carlo simulations. Statistical analysis was performed using R statistical software including meta-analysis of both populations of the cohort: African-Americans and Caucasians. Meta-analysis was performed using the "Meta" package, with fixed effects and continuous outcome data. Inverse variance weighting was used for pooling. The DerSimonian-Laird estimate for the between-study variance was used in the random-effects model by default. Statistical significance was calculated using Student's *t*-test or by one- or two-way ANOVA

with LSD *post hoc*, where appropriate; ± SEM is shown for all graphs.

Stereotactic injections

All experiments were approved by the ethics committee (IACUC) of The Hebrew University (approval #12-13528-4). Seven-eight-week-old male C57Bl/6J mice were group housed until they underwent stereotaxic surgery, after which they were singly housed, at a constant temperature (22 ± 1°C) and 12-h light/dark cycles. Mice were anesthetized by i.p. injections of ketamine (50 mg/kg; Forth Dodge, IA, USA) and Domitor (0.5 mg/kg; Orion Pharma, Espoo, Finland) mix and then mounted in a stereotaxic apparatus for intracerebroventricular injections (55). 10 μM ML141 (Tocris Bioscience, Bristol, UK) was injected intracerebroventricularly at the following coordinates (in mm) relative to bregma: AP: −0.46, ML: ±1 and DV: −2.2 mm. Bilateral injections of 1 μl were conducted using a 10 μl Glenco syringe (Huston, TX, USA). After each injection, the needle was left for 5 min before being slowly retracted to allow complete diffusion.

Behavioral analysis

Elevated plus maze

Anxiety-related behaviors were tested in a Plexiglas plus-shaped maze containing two dark and enclosed arms (30 × 5 cm with a 5 × 5 cm center area and 40 cm-high walls) and two 30 × 5 cm open and lit arms, all elevated 50 cm above ground. Individual mice were placed in the center of the maze, tracked for 5 min with a video camera and then returned to their home cage. The plus maze was wiped clean between trials with a 70% alcohol solution. Analysis was performed using EthoVision software and the Noldus system (Wageningen, The Netherlands).

Open field

Open field tests were performed in a square gray plastic arena (50 × 50 cm, 40 cm high). Mice were placed in the periphery of the arena, and their behavior was recorded for 5 min using a camera. Between trials, the surface of the arena was cleaned with 70% ethanol. Behavior was analyzed using EthoVision software and the Noldus system.

G-LISA

Levels of Cdc42-GTP were measured in mice hippocampi 24 h post-injection of the CDC42 inhibitor ML141 (42) using a G-LISA kit (BK127, Cytoskeleton, CO, USA) according to manufacturer's instructions. Positive controls included CDC42-GTP provided in the kit and negative controls included buffer-only samples. Repeated calibration experiments led to dose selection yielding 40% suppression of hippocampal CDC42-GTPase activity, mimicking the status of SNP minor allele humans.

SUPPLEMENTARY MATERIAL

Supplementary Material is available at *HMG* online.

ACKNOWLEDGEMENTS

The authors thank Drs David R. Bennett (Rush University's Medical Center, Chicago, IL, USA) and Michael T. Heneka (University of Bonn, Germany) for thoughtful comments, and those volunteers who donated tissues and personal details to the HERITAGE cohort and the Netherlands Brain Bank. Thanks are expressed to Drs Arthur S. Leon (University of Minneapolis, MN, USA), James S. Skinner (Indiana University, Indianapolis, IN, USA) and Jack H. Wilmore (University of Texas at Austin, Austin, Texas) who were involved in the planning and data collection of HERITAGE. The contribution of Dr Daniel M. Landers (Arizona State University, Tempe, AZ, USA) to the anxiety measurements is gratefully acknowledged.

Conflict of Interest statement. None declared.

FUNDING

Support of this study by the European Research Council (Advanced Award 321501, to H.S.) is acknowledged. S.S.-T. and N.Y. are supported by an Eshkol post-doctoral fellowship and an ELSC pre-doctoral fellowship. The HERITAGE Family Study was supported by grants from the National Institutes of Health (HL45670, HL47323, HL47317, HL47327 and HL47321). Funding to pay the Open Access publication charges for this article was provided by the Israel I-Core Trauma Center of Excellence.

REFERENCES

1. Bartel, D.P. (2009) MicroRNAs: target recognition and regulatory functions. *Cell*, **136**, 215–233.
2. Lau, P. and de Strooper, B. (2010) Dysregulated microRNAs in neurodegenerative disorders. *Semin. Cell. Dev. Biol.*, **21**, 768–773.
3. Filipowicz, W., Bhattacharyya, S.N. and Sonenberg, N. (2008) Mechanisms of post-transcriptional regulation by microRNAs: are the answers in sight? *Nat. rev. Genet.*, **9**, 102–114.
4. Shaked, I., Meerson, A., Wolf, Y., Avni, R., Greenberg, D., Gilboa-Geffen, A. and Soreq, H. (2009) MicroRNA-132 potentiates cholinergic anti-inflammatory signaling by targeting acetylcholinesterase. *Immunity*, **31**, 965–973.
5. Soreq, H. and Wolf, Y. (2011) NeurimmiRs: microRNAs in the neuroimmune interface. *Trends Mol. Med.*, **17**, 548–555.
6. Abelson, J.F., Kwan, K.Y., O'Roak, B.J., Baek, D.Y., Stillman, A.A., Morgan, T.M., Mathews, C.A., Pauls, D.L., Rasin, M.R., Gunel, M. *et al.* (2005) Sequence variants in SLITRK1 are associated with Tourette's syndrome. *Science*, **310**, 317–320.
7. Martin, M.M., Buckenberger, J.A., Jiang, J., Malana, G.E., Nuovo, G.J., Chotani, M., Feldman, D.S., Schmittgen, T.D. and Elton, T.S. (2007) The human angiotensin II type 1 receptor +1166 A/C polymorphism attenuates microrna-155 binding. *J. Biol. Chem.*, **282**, 24262–24269.
8. Poliseno, L., Salmena, L., Zhang, J., Carver, B., Haveman, W.J. and Pandolfi, P.P. (2010) A coding-independent function of gene and pseudogene mRNAs regulates tumour biology. *Nature*, **465**, 1033–1038.
9. Salmena, L., Poliseno, L., Tay, Y., Kats, L. and Pandolfi, P.P. (2011) A ceRNA hypothesis: the Rosetta Stone of a hidden RNA language? *Cell*, **146**, 353–358.
10. Tay, Y., Rinn, J. and Pandolfi, P.P. (2014) The multilayered complexity of ceRNA crosstalk and competition. *Nature*, **505**, 344–352.
11. Franco-Zorrilla, J.M., Valli, A., Todesco, M., Mateos, I., Puga, M.I., Rubio-Somoza, I., Leyva, A., Weigel, D., Garcia, J.A. and Paz-Ares, J. (2007) Target mimicry provides a new mechanism for regulation of microRNA activity. *Nat. Genet.*, **39**, 1033–1037.
12. Lau, P., Bossers, K., Salta, E., Sala Frigerio, C., Janky, R., Barbash, S., Rothman, R., Sierksma, A., Thathiah, A., Greenberg, D.S. *et al.* (2013) Alteration of the microRNA network during the progression of Alzheimer's disease. *Embo Mol. Med.*, **5**, 1613–1634.
13. Maharshak, N., Shenhar-Tsarfaty, S., Aroyo, N., Orpaz, N., Guberman, I., Canaani, J., Halpern, Z., Dotan, I., Berliner, S. and Soreq, H. (2013) MicroRNA-132 modulates cholinergic signaling and inflammation in human inflammatory bowel disease. *Inflamm. Bowel. Dis.*, **19**, 1346–1353.

14. Shaltiel, G., Hanan, M., Wolf, Y., Barbash, S., Kovalev, E., Shoham, S. and Soreq, H. (2013) Hippocampal microRNA-132 mediates stress-inducible cognitive deficits through its acetylcholinesterase target. *Brain Struct. Funct.*, **218**, 59–72.
15. Ryan, B.M., McClary, A.C., Valeri, N., Robinson, D., Paone, A., Bowman, E.D., Robles, A.I., Croce, C. and Harris, C.C. (2012) rs4919510 in hsa-mir-608 is associated with outcome but not risk of colorectal cancer. *PLoS ONE*, **7**, e36306.
16. Haramati, S., Navon, I., Issler, O., Ezra-Nevo, G., Gil, S., Zwang, R., Hornstein, E. and Chen, A. (2011) MicroRNA as repressors of stress-induced anxiety: the case of amygdalar miR-34. *J. Neurosci.*, **31**, 14191–14203.
17. Mineur, Y.S., Obayemi, A., Wigestrand, M.B., Fote, G.M., Calarco, C.A., Li, A.M. and Picciotto, M.R. (2013) Cholinergic signaling in the hippocampus regulates social stress resilience and anxiety- and depression-like behavior. *Proc. Natl. Acad. Sci. USA*, **110**, 3573–3578.
18. Hasin, Y., Avidan, N., Bercovich, D., Korczyn, A., Silman, I., Beckmann, J.S. and Sussman, J.L. (2004) A paradigm for single nucleotide polymorphism analysis: the case of the acetylcholinesterase gene. *Hum. Mutat.*, **24**, 408–416.
19. Jeyapalan, Z., Deng, Z., Shatseva, T., Fang, L., He, C. and Yang, B.B. (2011) Expression of CD44 3′-untranslated region regulates endogenous microRNA functions in tumorigenesis and angiogenesis. *Nucl. Acids Res.*, **39**, 3026–3041.
20. Kang, J.G., Majerciak, V., Uldrick, T.S., Wang, X., Kruhlak, M., Yarchoan, R. and Zheng, Z.M. (2011) Kaposi's sarcoma-associated herpesviral IL-6 and human IL-6 open reading frames contain miRNA binding sites and are subject to cellular miRNA regulation. *J. Pathol.*, **225**, 378–389.
21. Hanin, G. and Soreq, H. (2011) Cholinesterase-targeting microRNAs Identified in silico affect specific biological processes. *Frontiers Mol. Neurosci.*, **4**, 28.
22. Homola, J. (2008) Surface plasmon resonance sensors for detection of chemical and biological species. *Chem. Rev.*, **108**, 462–493.
23. Zhang, Y., Cheng, Y., Ren, X., Zhang, L., Yap, K.L., Wu, H., Patel, R., Liu, D., Qin, Z.H., Shih, I.M. *et al.* (2012) NAC1 modulates sensitivity of ovarian cancer cells to cisplatin by altering the HMGB1-mediated autophagic response. *Oncogene*, **31**, 1055–1064.
24. Guhaniyogi, J., Sohar, I., Das, K., Stock, A.M. and Lobel, P. (2009) Crystal structure and autoactivation pathway of the precursor form of human tripeptidyl-peptidase 1, the enzyme deficient in late infantile ceroid lipofuscinosis. *J. Biol. Chem.*, **284**, 3985–3997.
25. Papadopoulos, T., Korte, M., Eulenburg, V., Kubota, H., Retiounskaia, M., Harvey, R.J., Harvey, K., O'Sullivan, G.A., Laube, B., Hulsmann, S. *et al.* (2007) Impaired GABAergic transmission and altered hippocampal synaptic plasticity in collybistin-deficient mice. *EMBO J.*, **26**, 3888–3899.
26. Vallieres, L., Campbell, I.L., Gage, F.H. and Sawchenko, P.E. (2002) Reduced hippocampal neurogenesis in adult transgenic mice with chronic astrocytic production of interleukin-6. *J. Neurosci.*, **22**, 486–492.
27. Raison, C.L. and Miller, A.H. (2012) The evolutionary significance of depression in pathogen host defense (PATHOS-D). *Mol. Psychiatry*, **18**, 15–37.
28. Berson, A., Barbash, S., Shaltiel, G., Goll, Y., Hanin, G., Greenberg, D.S., Ketzef, M., Becker, A.J., Friedman, A. and Soreq, H. (2012) Cholinergic-associated loss of hnRNP-A/B in Alzheimer's disease impairs cortical splicing and cognitive function in mice. *EMBO Mol. Med.*, **4**, 730–742.
29. Podoly, E., Shalev, D.E., Shenhar-Tsarfaty, S., Bennett, E.R., Ben Assayag, E., Wilgus, H., Livnah, O. and Soreq, H. (2009) The butyrylcholinesterase K variant confers structurally derived risks for Alzheimer pathology. *J. Biol. Chem.*, **284**, 17170–17179.
30. Pavlov, V.A., Parrish, W.R., Rosas-Ballina, M., Ochani, M., Puerta, M., Ochani, K., Chavan, S., Al-Abed, Y. and Tracey, K.J. (2009) Brain acetylcholinesterase activity controls systemic cytokine levels through the cholinergic anti-inflammatory pathway. *Brain Behav. Immun.*, **23**, 41–45.
31. Rosas-Ballina, M., Olofsson, P.S., Ochani, M., Valdes-Ferrer, S.I., Levine, Y.A., Reardon, C., Tusche, M.W., Pavlov, V.A., Andersson, U., Chavan, S. *et al.* (2011) Acetylcholine-synthesizing T cells relay neural signals in a vagus nerve circuit. *Science*, **334**, 98–101.
32. O'Donovan, A., Hughes, B.M., Slavich, G.M., Lynch, L., Cronin, M.T., O'Farrelly, C. and Malone, K.M. (2010) Clinical anxiety, cortisol and interleukin-6: evidence for specificity in emotion-biology relationships. *Brain Behav. Immun.*, **24**, 1074–1077.
33. Kaufer, D., Friedman, A., Seidman, S. and Soreq, H. (1998) Acute stress facilitates long-lasting changes in cholinergic gene expression. *Nature*, **393**, 373–377.
34. Tyagarajan, S.K., Ghosh, H., Harvey, K. and Fritschy, J.M. (2011) Collybistin splice variants differentially interact with gephyrin and Cdc42 to regulate gephyrin clustering at GABAergic synapses. *J. Cell Sci.*, **124**, 2786–2796.
35. Guyenet, P.G. (2006) The sympathetic control of blood pressure. *Nat. Rev. Neurosci.*, **7**, 335–346.
36. Sklan, E.H., Lowenthal, A., Korner, M., Ritov, Y., Landers, D.M., Rankinen, T., Bouchard, C., Leon, A.S., Rice, T., Rao, D.C. *et al.* (2004) Acetylcholinesterase/paraoxonase genotype and expression predict anxiety scores in Health, Risk Factors, Exercise Training, and Genetics study. *Proc. Natl. Acad. Sci. USA*, **101**, 5512–5517.
37. Gershon, E.S., Badner, J.A., Goldin, L.R., Sanders, A.R., Cravchik, A. and Detera-Wadleigh, S.D. (1998) Closing in on genes for manic-depressive illness and schizophrenia. *Neuropsychopharmacology*, **18**, 233–242.
38. Miwa, J.M., Freedman, R. and Lester, H.A. (2011) Neural systems governed by nicotinic acetylcholine receptors: emerging hypotheses. *Neuron*, **70**, 20–33.
39. Yehuda, R. and Seckl, J. (2011) Minireview: stress-related psychiatric disorders with low cortisol levels: a metabolic hypothesis. *Endocrinology*, **152**, 4496–4503.
40. Ong, K.L., Cheung, B.M., Man, Y.B., Lau, C.P. and Lam, K.S. (2007) Prevalence, awareness, treatment, and control of hypertension among United States adults 1999–2004. *Hypertension*, **49**, 69–75.
41. Lettre, G., Palmer, C.D., Young, T., Ejebe, K.G., Allayee, H., Benjamin, E.J., Bennett, F., Bowden, D.W., Chakravarti, A., Dreisbach, A. *et al.* (2011) Genome-wide association study of coronary heart disease and its risk factors in 8,090 African Americans: the NHLBI CARe Project. *PLoS Genet.*, **7**, e1001300.
42. Martin-Granados, C., Prescott, A.R., Van Dessel, N., Van Eynde, A., Arocena, M., Klaska, I.P., Gornemann, J., Beullens, M., Bollen, M., Forrester, J.V. *et al.* (2012) A role for PP1/NIPP1 in steering migration of human cancer cells. *PLoS ONE*, **7**, e40769.
43. Barbash, S., Shifman, S. and Soreq, H. (In Press) Global co-evolution of human microRNAs and their target genes. *Mol. Biol. Evol.*, doi:10.1093/molbev/msu090.
44. Nadorp, B. and Soreq, H. (2014) Predicted overlapping microRNA regulators of acetylcholine packaging and degradation in neuroinflammation-related disorders. *Frontiers Mol. Neurosci.*, **7**, in press.
45. Akiguchi, I. and Yamamoto, Y. (2010) Vascular mechanisms of cognitive impairment: roles of hypertension and subsequent small vessel disease under sympathetic influences. *Hypertens Res.*, **33**, 29–31.
46. McEwen, B.S. and Gianaros, P.J. (2011) Stress- and allostasis-induced brain plasticity. *Annu. Rev. Med.*, **62**, 431–445.
47. Deter, H.C., Micus, C., Wagner, M., Sharma, A.M. and Buchholz, K. (2006) Salt sensitivity, anxiety, and irritability predict blood pressure increase over five years in healthy males. *Clin. Exp. Hypertens*, **28**, 17–27.
48. Schneider, G.M., Jacobs, D.W., Gevirtz, R.N. and O'Connor, D.T. (2003) Cardiovascular haemodynamic response to repeated mental stress in normotensive subjects at genetic risk of hypertension: evidence of enhanced reactivity, blunted adaptation, and delayed recovery. *J. Hum. Hypertens*, **17**, 829–840.
49. Gianaros, P.J., Onyewuenyi, I.C., Sheu, L.K., Christie, I.C. and Critchley, H.D. (2012) Brain systems for baroreflex suppression during stress in humans. *Hum. Brain Mapp.*, **33**, 1700–1716.
50. Gianaros, P.J., Sheu, L.K., Remo, A.M., Christie, I.C., Crtichley, H.D. and Wang, J. (2009) Heightened resting neural activity predicts exaggerated stressor-evoked blood pressure reactivity. *Hypertension*, **53**, 819–825.
51. Jennings, J.R. and Zanstra, Y. (2009) Is the brain the essential in hypertension? *Neuroimage*, **47**, 914–921.
52. Stranahan, A.M. and Mattson, M.P. (2012) Recruiting adaptive cellular stress responses for successful brain ageing. *Nat. Rev. Neurosci.*, **13**, 209–216.
53. Ofek, K., Krabbe, K.S., Evron, T., Debecco, M., Nielsen, A.R., Brunnsgaad, H., Yirmiya, R., Soreq, H. and Pedersen, B.K. (2007) Cholinergic status modulations in human volunteers under acute inflammation. *J. Mol. Med. (Berl)*, **85**, 1239–1251.
54. Peritz, T., Zeng, F., Kannanayakal, T.J., Kilk, K., Eiriksdottir, E., Langel, U. and Eberwine, J. (2006) Immunoprecipitation of mRNA-protein complexes. *Nat. Protoc.*, **1**, 577–580.
55. Barbash, S., Hanin, G. and Soreq, H. (2013) Stereotactic injection of microRNA-expressing lentiviruses to the mouse hippocampus ca1 region and assessment of the behavioral outcome. *J. Vis. Exp.*, **76**, e50170.